Synthesis and Analysis of State-Space Active Filters Using Intermediate Transfer Functions

W. MARTIN SNELGROVE AND ADEL S. SEDRA, FELLOW, IEEE

Abstract—**This paper is concerned with the realization of a given arbitrary filter transfer function as a network of resistively interconnected integrators. These state-space realizations are synthesized using a new technique called intermediate function (IF) synthesis. The technique is based on the selection of a set of functions to serve as either the transfer functions from the filter input to the integrator outputs or the transfer functions from the integrator inputs to the filter output. Relationships between the filter sensitivity and dynamic range and the intermediate functions are derived. A number of results are also given to aid in the selection of a set of IF's that yields structures with optimum performance.**

I. Introduction

IN THE VLSI era, as mixed analog/digital circuitry of increasing complexity is implemented on a single IC chip, the need becomes even greater for analog filter realizations that have very low sensitivities and, most importantly, low-noise performance. In fact, it appears that noise is the major problem with the currently popular approach for implementing monolithic filters, namely the switched-capacitor technique [1].

Structures for filters suitable in a VLSI environment are likely to consist of a number of identical operator blocks, e.g., integrators, connected together with feedback and feedforward networks [2]. Each such operator block could be implemented by a very simple circuit, for instance integrators could be realized as simple controlled current-sources feeding capacitors. On the other hand, the feedback network could be extensive, and designed so as to make the overall sensitivities and noise very small.

Motivated by this philosophy, this paper presents a new technique for the synthesis and analysis of analog filters. The method is concerned with the realization of a given nth order transfer function $t(s)$ with a structure of n resistively interconnected integrators. It will be shown that the design process consists of two steps: 1) selection of a set of n functions, called *intermediate transfer functions* (IFs) from the given $t(s)$; and 2) synthesis of a circuit realization of $t(s)$ from the selected IF's. Because, as will be seen, the second step is quite straightforward, the design effort can be concentrated on the first, namely the selection of a "good" set of IF's.

Manuscript received October 17, 1984; revised August 1, 1985. This work was supported by the Natural Sciences and Engineering Research Council of Canada under Grant A7394.

The authors are with the Department of Electrical Engineering, University of Toronto, Toronto, Ont. M5S 1A4, Canada.

IEEE Log Number 8406681.

The major advantage of the proposed method is that the IF's can be very effectively employed in determining the expected sensitivity and dynamic range performance of the active filter; a "good" set of IF's is obviously one that optimizes these performance measures. Of particular significance here is that performance evaluation and optimization is performed not at the level of circuit topology but at the more abstract level of IF's and thus at a very early stage in the design process. It should also be pointed out that, unlike earlier attempts in this direction [3], the proposed method does not rely on numerical optimization techniques, and thus affords greater insight inoto the properties of "good" filter structures.

In Section II we define the IF's and present the synthesis method. The use of IFs in sensitivity analysis is described in Section III. Their application to dynamic range analysis, scaling, and optimization is the subject of Section IV. In Section V the IF method is employed in the synthesis and structural study of a number of old and new filter realizations.

II. Intermediate Function Synthesis

A. State-Space Description

As mentioned above we are interested in the realization of an nth-order active filter as a structure of n resistively interconnected integrators. Such a system is most conveniently described by the state-variable formulation [4], [5]

$$s\boldsymbol{x}(s) = \boldsymbol{A}\boldsymbol{x}(s) + \boldsymbol{b}u(s) \tag{1}$$

$$y(s) = \boldsymbol{c}^T\boldsymbol{x}(s) + du(s) \tag{2}$$

where the vector $\boldsymbol{x}(s)$ represents the circuit states (integrator outputs), the matrix $\boldsymbol{A}$ describes the interconnection (feedback and feedforward paths) of the n integrators, the vector $\boldsymbol{b}$ contains the coefficients that multiply the input signal $u(s)$ as it is applied to the inputs of the integrators, the vector $\boldsymbol{c}$ contains the coefficients required to form the output $y(s)$ as a weighted sum of the n states, and the scalar d is the coefficient of the feedthrough component from input to output.

Given a set $\{\boldsymbol{A}, \boldsymbol{b}, \boldsymbol{c}, d\}$ one can easily obtain a variety of active circuit realizations. In this paper we shall be specifically interested in realizations that maintain a direct correspondence between the system coefficients (that is,

elements of A, b, c and d) and the circuit component values. Such a realization will be referred to as a *state-space filter*.

The transfer function of the filter described by (1) and (2) is

$$t(s) \triangleq \frac{y(s)}{u(s)} = c^T(sI - A)^{-1}b + d \triangleq \frac{p(s)}{e(s)} \tag{3}$$

where $e(s)$ is the natural mode (pole) polynomial (of order n) and $p(s)$ is the transmission zero polynomial (of order $\leqslant n$).

B. Intermediate Transfer Functions

We define two dual sets of intermediate transfer functions: $\{f_i(s)\}$ and $\{g_i(s)\}$. The first set, $\{f_i(s)\}$, contains the transfer functions from the filter input to the integrator outputs

$$f_i(s) \triangleq \frac{x_i(s)}{u(s)}.$$

Using (1) one can show that the vector $f(s)$ that contains the $f_i(s)$ functions is given by

$$f(s) = (sI - A)^{-1}b. \tag{4}$$

The second set of intermediate functions, $\{g_i(s)\}$, contains the transfer functions from integrator inputs to the filter output

$$g_i(s) \triangleq \frac{y(s)}{\epsilon_i(s)} \tag{5}$$

where $\epsilon_i(s)$ is the ith component of a vector of auxiliary input signals injected at integrator inputs according to

$$sx(s) = Ax(s) + bu(s) + \epsilon(s). \tag{6}$$

Since $\epsilon_i(s)$ can model the noise generated at the input of the ith integrator, $g_i(s)$ can be physically interpreted as the noise gain of integrator i. We will occasionally refer to the functions $\{g_i(s)\}$ as noise gains and to $\{f_i(s)\}$ as signal gains. These interpretations will be found especially meaningful in the context of dynamic range analysis in Section IV.

From the definitions of the g functions in (5) and using (6) together with (2) while setting $u(s) = 0$, the vector $g(s)$ can be obtained as

$$g^T(s) = c^T(sI - A)^{-1}. \tag{7}$$

From (3), (4) and (7) we observe that $t(s)$, $\{f_i(s)\}$ and $\{g_i(s)\}$ all have the same poles, the roots $e_1, e_2, \cdots, e_n$ of the natural mode polynomial $e(s) = \det(sI - A)$. Now selecting the vector $v(s)$ where

$$v_i(s) = \frac{1}{s - e_i} \tag{8}$$

as a basis for expressing functions in an n-dimensional vector space we can write[1]

$$t(s) = t^T v(s) + t_{n+1} \tag{9}$$

$$f(s) = Fv(s) \tag{10}$$

$$g(s) = Gv(s) \tag{11}$$

where t is a vector containing the n residues of $t(s)$ at the poles and t_{n+1} is the residue at $s = \infty$ (in other words, (9) is a partial fraction expansion of $t(s)$), F is a matrix containing the residues of the f functions evaluated at the poles, and G is a matrix of the residues of the g functions. The elements of t, F and G are in general complex numbers.

The representations in (9), (10) and (11) enable the derivation of the following novel expressions which give the system parameters $\{A, b, c, d\}$ in terms of the f functions, and thus represent the essential step in the synthesis procedure that will be described shortly

$$A = FEF^{-1} \tag{12}$$

$$b = F\mathbf{1} \tag{13}$$

$$c^T = t^T F^{-1} \tag{14}$$

$$d = t_{n+1}. \tag{15}$$

Here E is a diagonal matrix having the natural modes $e_1, e_2, \cdots, e_n$ as its elements and $\mathbf{1} = (1\ 1 \cdots 1)^T$.

Finally we can derive the following simple formula relating F and G:

$$G^T = HF^{-1} \tag{16}$$

where H is a diagonal matrix formed from the residues of $t(s)$, i.e., $H = \mathrm{diag}(t_1, t_2, \cdots, t_n)$. This equation shows that G is inversely related to F and directly to $t(s)$. It will be seen later that this relationship has significant implications concerning filter performance.

To help in visualizing the structure of state-space filters we show in Fig. 1 their signal flow-graph representation, with the intermediate transfer functions indicated with broken lines.

C. IF Synthesis

Given a transfer function $t(s)$, IF synthesis is based on choosing a set of linearly independent functions, all having the same denominator polynomial $e(s)$ and arbitrary numerator polynomials of degree less than n. This set of functions can serve as $\{f_i(s)\}$ and from it we can obtain the $\{A, b, c, d\}$ parameters of a unique canonic realization using (12)–(15). The g functions of this realization can be evaluated using (16) and together with the f functions can be used to determine the expected performance of the realization, as will be outlined in the next two sections. Finally, note that rather than starting the synthesis with a set of f functions we may start with a set of g functions

[1]We assume that $e(s)$ has no repeated roots. This is a reasonable assumption to make for filter circuits. This assumption could be removed, at some cost to the clarity of the development and simplicity of the formulas.

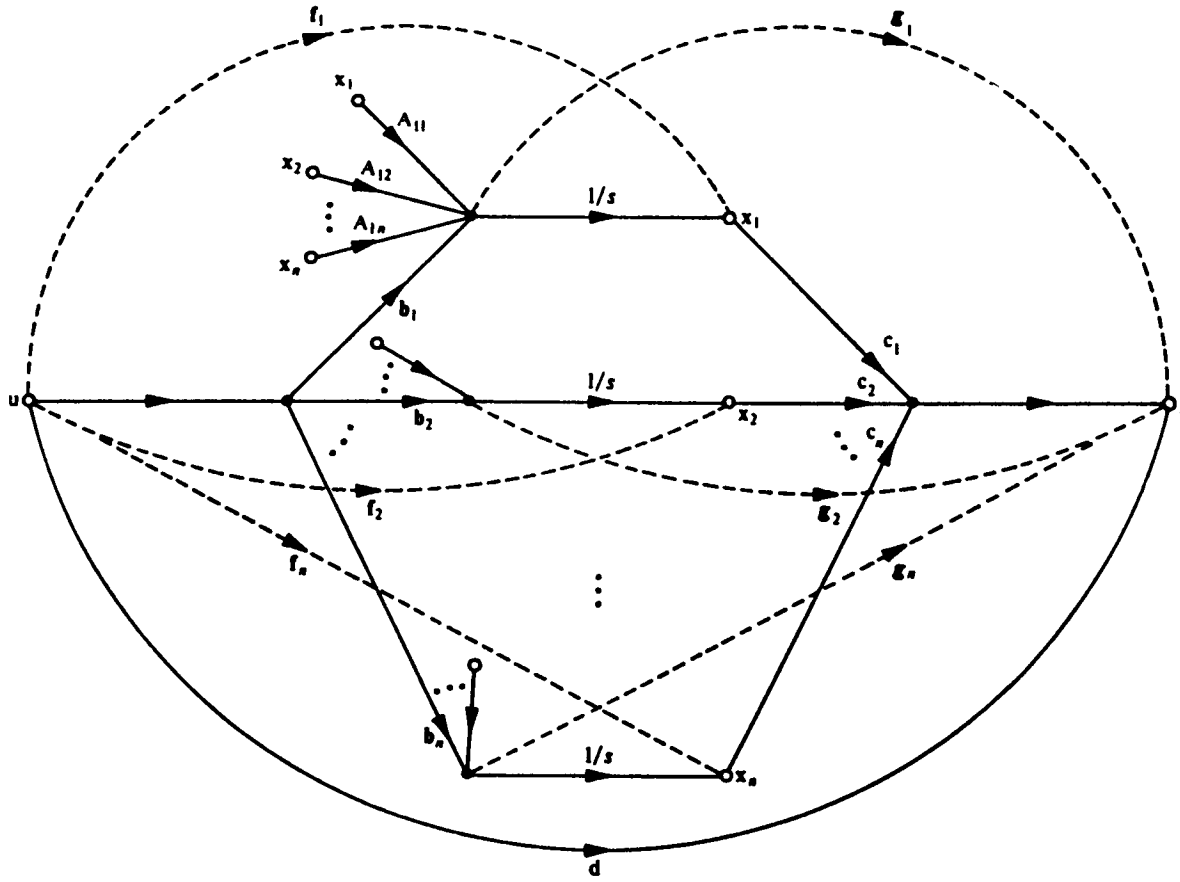

Fig. 1. Signal flowgraph of general system of state equations.

which must satisfy similar requirements as those stated above for the f functions.

The requirement of linear independence follows from the fact that a canonical realization must have n independent states; otherwise one or more of the integrators would be redundant and one could obtain a realization with less than n integrators; a clearly impossible task. Mathematically, if the IFs were not independent the matrix $\boldsymbol{F}$ would not be invertible and (12)–(15) could not be used to determine $\{\boldsymbol{A}, \boldsymbol{b}, \boldsymbol{c}, d\}$.

The requirement that the numerator order must be less than n follows from the fact that $\{f_i\}$ are transfer functions to integrator outputs and thus must have at least one transmission zero at $s=\infty$. Within these constraints the choice of n functions to serve as IF's is arbitrary. Clearly, however, the choice must be made with a view to optimizing performance. Indeed it is the fact that filter performance can be directly related to IFs that makes this synthesis method attractive.

To illustrate the IF synthesis method let us consider a simple example, namely the second-order Butterworth transfer function

$$t(s)=1/(s^2+\sqrt{2}s+1).$$

We may arbitrarily choose as intermediate functions

$$f_1(s)=1/e(s) \quad \text{and} \quad f_2(s)=s/e(s)$$

where

$$e(s)=s^2+\sqrt{2}s+1$$
$$=\left(s+\frac{1}{\sqrt{2}}-j\frac{1}{\sqrt{2}}\right)\left(s+\frac{1}{\sqrt{2}}+j\frac{1}{\sqrt{2}}\right).$$

Thus

$$e_1=-\frac{1}{\sqrt{2}}+j\frac{1}{\sqrt{2}} \quad \text{and} \quad e_2=-\frac{1}{\sqrt{2}}-j\frac{1}{\sqrt{2}}.$$

We also have

$$v(s)=\left(\frac{1}{s-e_1}\ \frac{1}{s-e_2}\right)^T$$
$$t=\left(-j/\sqrt{2} \quad j/\sqrt{2}\right)^T$$
$$t_{n+1}=0$$
$$\boldsymbol{F}=\begin{bmatrix} -j/\sqrt{2} & j/\sqrt{2} \\ \frac{1}{2}(1+j) & \frac{1}{2}(1-j) \end{bmatrix}.$$

Substituting in (12)–(15) yields

$$\boldsymbol{A}=\begin{bmatrix} 0 & 1 \\ -1 & -\sqrt{2} \end{bmatrix} \quad \boldsymbol{b}=[0 \quad 1]^T$$
$$\boldsymbol{c}^T=[1 \quad 0] \quad d=0.$$

Also

$$\boldsymbol{H}=\begin{bmatrix} -j/\sqrt{2} & 0 \\ 0 & j/\sqrt{2} \end{bmatrix}.$$

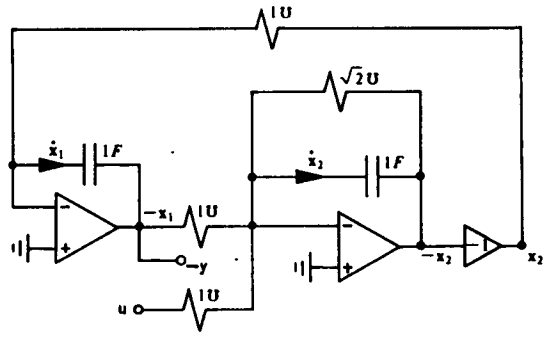

Fig. 2. Circuit implementation of the second-order state-space filter example.

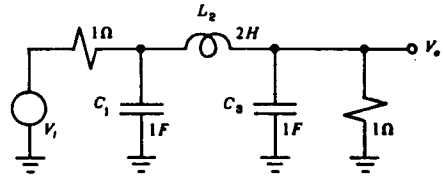

Fig. 3. *LC* circuit to be simulated.

Thus substituting in (16) gives

$$\boldsymbol{G}^T = \begin{bmatrix} \frac{1}{2}(1-j) & \frac{-j}{\sqrt{2}} \\ \frac{1}{2}(1+j) & \frac{j}{\sqrt{2}} \end{bmatrix}$$

from which the g functions are obtained as

$$g_1(s) = (s+\sqrt{2})/e(s) \quad \text{and} \quad g_2(s) = 1/e(s).$$

It should be noted that because this is a low-order example, the $\{\boldsymbol{A}, \boldsymbol{b}, \boldsymbol{c}, d\}$ elements could have been more easily obtained by substituting the selected $\{f_i\}$ in the state equations and employing coefficient matching [6]. We have chosen, however, to use the matrix formulas in order to illustrate their application and because computer programs implementing IF synthesis can use them.

Once $\{\boldsymbol{A}, \boldsymbol{b}, \boldsymbol{c}, d\}$ are determined one can easily derive a state-space circuit realization. As an example, using op-amp integrators we obtain the circuit in Fig. 2 for the Butterworth filter. This circuit can be easily recognized as the Tow–Thomas state-variable biquad [7], [8].

As another example, let it be required to design a state-space filter that simulates the operation of the third-order doubly terminated *LC* ladder network shown in Fig. 3. To achieve this simulation, the f functions must be chosen so that the state variables of the active filter are analogs of those of the *LC* ladder which are the capacitor voltages and inductor currents. It follows that

$$f_1(s) = \frac{V_{C1}(s)}{V_i(s)}$$

$$f_2(s) = \frac{I_{L2}(s)}{V_i(s)}$$

$$f_3(s) = \frac{V_{C3}(s)}{V_i(s)}.$$

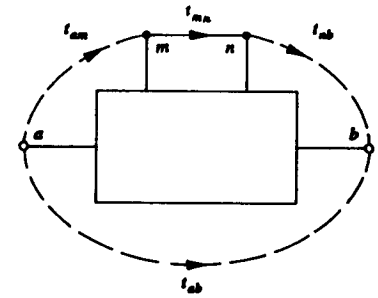

Fig. 4. Investigating the sensitivity to the transmittance t_{mn}.

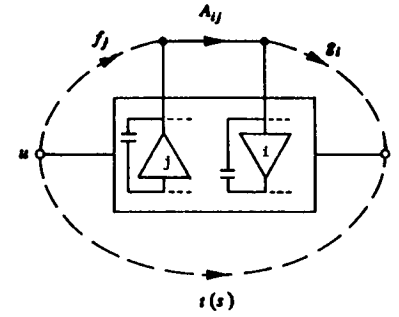

Fig. 5. Derivation of the sensitivity to A_{ij}.

These functions can be obtained from ladder analysis and $\{\boldsymbol{A}, \boldsymbol{b}, \boldsymbol{c}, d\}$ can then be determined using (12)–(15). The result is

$$\boldsymbol{A} = \begin{bmatrix} -1 & 1 & 0 \\ -0.5 & 0 & 0.5 \\ 0 & -1 & -1 \end{bmatrix} \qquad \boldsymbol{b} = \begin{bmatrix} 1 \\ 0 \\ 0 \end{bmatrix}$$

$$\boldsymbol{c}^T = [0 \quad 0 \quad 1] \qquad d = 0.$$

Note the tridiagonal structure of $\boldsymbol{A}$ which is a result of the ladder topology [9]. Obviously, this particular design could have been obtained using well known techniques [10]. IF synthesis, however, is capable of handling more complicated cases and of accurately predicting performance, as shown below.

III. Sensitivity

In this section we show how the f and g functions can be used to predict the sensitivity performance of state-space filters. Specifically, expressions will be derived for the sensitivities of the transfer function $t(s)$ to the state-space system parameters $\{\boldsymbol{A}, \boldsymbol{b}, \boldsymbol{c}, d\}$ and to errors in the transfer functions of the integrators. These results follow as a direct application of a well known formula originally derived in [11] using Tellegen's theorem. This formula relates the change in the transfer function of a system to the change in the transfer function of one of its constituent blocks. Specifically, for the system represented by the signal flow-graph in Fig. 4 we have

$$\frac{dt_{ab}}{dt_{mn}} = t_{am} t_{nb}. \tag{17}$$

To find the sensitivities of $t(s)$ relative to the elements of the $\boldsymbol{A}$ matrix consider Fig. 5 which shows how the output of the integrator j is applied to the input of

integrator i. Comparing this to the graph in Fig. 4 enables us to use the formula in (17) to obtain

$$\frac{\partial t(s)}{\partial A_{ij}} = g_i(s) f_j(s). \tag{18}$$

The classical sensitivity function

$$S_{A_{ij}}^{t(s)} \triangleq \frac{\partial t(s)}{\partial A_{ij}} \frac{A_{ij}}{t(s)}$$

can now be found as

$$S_{A_{ij}}^{t(s)} = g_i(s) f_j(s) \frac{A_{ij}}{t(s)}. \tag{19}$$

In a similar way we can find the sensitivities to the $\boldsymbol{b}$, $\boldsymbol{c}$ and d elements as

$$S_{b_i}^{t(s)} = g_i(s) \frac{b_i}{t(s)} \tag{20}$$

$$S_{c_i}^{t(s)} = f_i(s) \frac{c_i}{t(s)} \tag{21}$$

$$S_{d}^{t(s)} = \frac{d}{t(s)}. \tag{22}$$

Since state-space filter implementations maintain a direct correspondence between circuit components and elements of the $\{\boldsymbol{A}, \boldsymbol{b}, \boldsymbol{c}, d\}$ system, it follows that the formulas in (19)–(22) do in fact give the sensitivities of the transfer function $t(s)$ to the conductance values of the resistors that interconnect the integrators. It now remains to find the sensitivities relative to the transfer functions of the integrators. Toward that end consider the situation depicted in Fig. 6. Here we have lumped the errors in the transfer function of integrator i in a single block having a transfer function $\gamma_i(s)$ and placed in cascade with an ideal integrator. The function $\gamma_i(s)$ includes the error in the integrator transfer function caused by changes in the value of the integrator capacitor as well as those errors caused by the finite gain and limited bandwidth of the integrator op amp (if an op amp realization is used). Nominally $\gamma_i(s) = 1$. Now comparing Figs. 6 and 4 we see that $t_{am} = f_i(s)$ and $t_{nb} = s g_i(s)$. Thus

$$S_{\gamma_i(s)}^{t(s)} = f_i(s) g_i(s) \frac{s}{t(s)}. \tag{23}$$

Since the integrator gain is inversely proportional to the value of its capacitor it follows that the sensitivity to the capacitor value is just the negative of the value given by (23). The sensitivity function given by (23) can also be used to find the effects of the finite gain and bandwidth of the op amp by deriving an expression for $\gamma_i(s)$ in terms of op amp gain $\mu_i(s)$ and using

$$S_{\mu_i(s)}^{t(s)} = S_{\gamma_i(s)}^{t(s)} S_{\mu_i(s)}^{\gamma_i(s)}. \tag{24}$$

We shall not carry out this development here any further except to note that $S_{\mu_i(s)}^{\gamma_i(s)}$ is dependent on the integrator gain or equivalently on its effective time constant; the greater the gain required from an integrator the larger the sensitivity to its op amp nonidealities. In terms of $\{\boldsymbol{A}, \boldsymbol{b}, \boldsymbol{c}, d\}$ elements the gain of integrator i is proportional to the row sum

$$\left[\sum_{j=1}^{n} |A_{ij}| + |b_i| \right].$$

It follows that realizations in which these row sums are large exhibit increased sensitivities to op amp nonidealities. On the other hand, "good" realizations have row sums that are almost equal and small in value, as demonstrated by the examples of Section V.

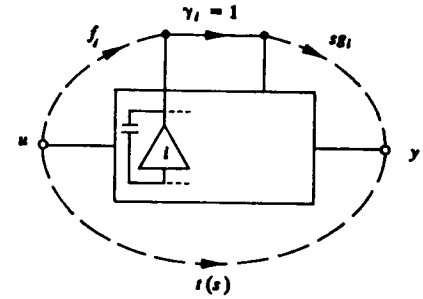

Fig. 6. Derivation of the sensitivity to the ith integrator.

As an example of the application of the sensitivity formulas above consider the third-order state-space filter designed in Section II. Its $\{f_i\}$ and $\{g_i\}$ are

$$\begin{aligned} f_1(s) &= g_3(s) \\ &= (s+0.5+j0.5)(s+0.5-j0.5)/e(s) \\ f_2(s) &= 0.5(s+1)/e(s) \\ f_3(s) &= g_1(s) = 0.5/e(s) \\ g_2(s) &= -(s+1)/e(s) \end{aligned}$$

where

$$\begin{aligned} t(s) &= \frac{p(s)}{e(s)} \\ &= \frac{0.5}{(s+1)(s+0.5+j0.866)(s+0.5-j0.866)}. \end{aligned}$$

We can use (19) to find that, e.g.

$$\begin{aligned} S_{A_{11}}^{t(s)} &= g_1 f_1 \frac{A_{11}}{t(s)} \\ &= \frac{-0.5(s+0.5+j0.5)(s+0.5-j0.5)}{p(s)e(s)}. \end{aligned}$$

Plots showing $|S_{A_{11}}^{t(j\omega)}|$ and $\mathrm{Re}[S_{A_{11}}^{t(j\omega)}] \equiv S_{A_{11}}^{|t(j\omega)|}$ appear in Fig. 7. Inspection of the curve for $S_{A_{11}}^{|t|}$ reveals a maximum value of about 0.75 near $s = j1$, the passband edge. This may be interpreted according to the formula [10]

$$\begin{aligned} \Delta\,\text{Attenuation}(\omega) &\simeq 8.68 \frac{\Delta|t|}{|t|} \\ &= 8.68 S_{A_{11}}^{|t|} \frac{\Delta A_{11}}{A_{11}}, \qquad \text{in decibels} \end{aligned}$$

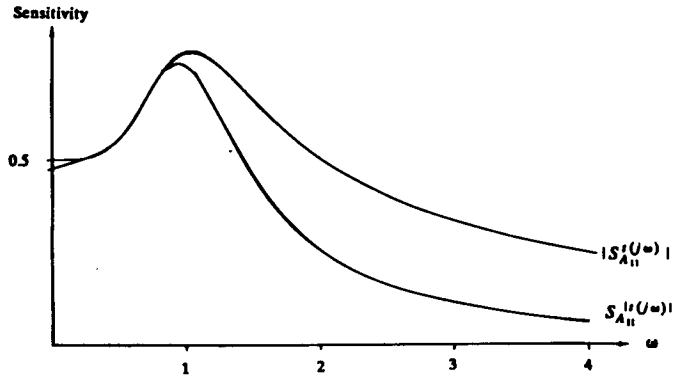

Fig. 7. Sensitivity of the ladder simulation circuit to A_{11}.

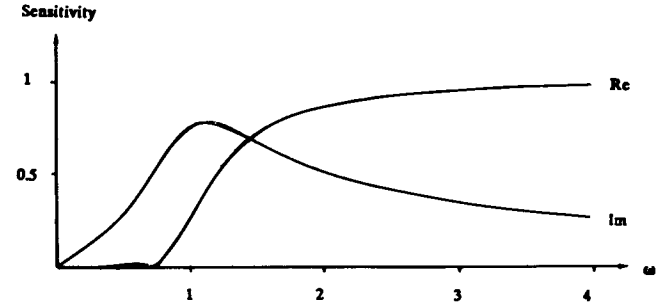

Fig. 8. Sensitivity of the magnitude of the transfer function of the *LC* ladder simulation circuit to the magnitude and phase of the first integrator.

to find that a 1 percent error in A_{11} causes a 0.065 dB error at the passband edge.

Because for this ladder network we have $f_1 = g_3$ and $f_3 = g_1$ then $f_1 g_1 = f_3 g_3$ which results in $S_{A_{11}}^{t(s)} = S_{A_{33}}^{t(s)}$; that is, errors in the ladder terminations have identical effects.

Fig. 8 shows plots of the real and imaginary parts of integrator sensitivities $S_{\gamma_i}^{t(s)}$ for integrators 1 and 3 (which are equal because $f_1 g_1 = f_3 g_3$). The real and imaginary parts of the sensitivity function measure, respectively, the sensitivities of $|t|$ to gain and phase errors in integrators. Note the low sensitivity of $|t|$ in the passband, which goes to zero at the reflection zeros. Thus the active filter has the same sensitivity properties as those predicted by Orchard [12] for the *LC* ladder being simulated.

The individual sensitivity values evaluated using the formulas above can of course be combined together to form any desired multiparameter sensitivity figure [13]. We shall not, however, pursue the subject of aggregate sensitivity measures here. Rather, we shall conclude this study of sensitivity of state-space filters by considering the question of minimizing the sensitivity of the filter to its integrators. Although optimizing sensitivity to integrators addresses only part of the general problem of designing a good filter it appears to be an important part for two reasons. Firstly, integrators are often the "weak link." Secondly, designs insensitive to their integrators appear to have good dynamic range, low component spreads, and low sensitivities to system coefficients in general. As an example, we observe that the good sensitivity behavior of *LC* ladders with respect to their reactive components at reflection zeros can be seen as guaranteeing good performance with respect to the ladder "integrators;" the *LC* components. Design by ladder simulation seeks to maintain the same low sensitivities to active-*RC* integrators. Thus a good solution to the problem of minimizing integrator sensitivities should be at least as good as *LC* simulation.

The following important sensitivity invariant which is useful for sensitivity minimization can be derived [14]

$$\sum_i f_i(s) g_i(s) = -\frac{dt(s)}{ds}. \tag{25}$$

In words, the sum over all products $f_i(s)g_i(s)$ is independent of the realization. Combining (23) and (25) we obtain a classical sensitivity result

$$\sum_i S_{\gamma_i}^{t(s)} = -\frac{s}{t(s)}\frac{dt(s)}{ds}. \tag{26}$$

Now suppose we wish to minimize an aggregate measure of integrator sensitivity of the form $\sum_i |S_{\gamma_i}^{t(s)}|^p$ with $p \geq 1$. Because the sum of the sensitivities is constant (equation (26)) it follows that the minimum is obtained when all sensitivities are equal. We therefore seek the realization (if it exists) for which, for all i

$$S_{\gamma_i}^{t(s)} = -\frac{1}{n}\frac{s}{t(s)}\frac{dt(s)}{ds}. \tag{27}$$

This represents a lower bound on integrator sensitivity. Using (27) together with (23) yields for the minimum-sensitivity realization

$$f_i(s) g_i(s) = -\frac{1}{n}\frac{dt(s)}{ds} \qquad \forall i. \tag{28}$$

Application of this formula to the second-order case was given in [15]. For higher orders this minimum-sensitivity realization is attainable only in special cases. It is possible, however, to obtain realizations that are "close" to this minimum (Section V). Finally, it should be mentioned that in studying the integrator sensitivities of a given realization more insight is gained by normalizing these sensitivity figures relative to those for the minimum-sensitivity realization. Specifically, in Section V we shall use the function

$$S_{\gamma_i}(\omega) = \left| \frac{f_i(j\omega) g_i(j\omega)}{[dt(j\omega)/d\omega]} \right|. \tag{29}$$

This normalized measure of integrator sensitivity enables one to see how close a design is to being optimum: The optimum design, if it exists, would have $S_{\gamma_i}(\omega) = 1/n$ $\forall i, \omega$. To further simplify sensitivity comparisons we shall frequently use the worst-case function

$$S_{\gamma,\infty}(\omega) = \max_i S_{\gamma_i}(\omega). \tag{30}$$

Here the subscript ∞ notes an L_∞ norm.

IV. Dynamic Range

Dynamic range is the ratio of the largest to the smallest signal that the filter can accommodate. While the largest signal is usually determined by amplifier saturation or

slew-rate limiting, the smallest useful signal is determined by electrical noise. Dynamic range has been thoroughly studied for digital filters [16]. In this section we present results on the dynamic range of the less extensively studied analog case. Of special interest is the relationship of dynamic range to the intermediate functions of IF synthesis. We will be interested in three problems: analysis of a design to find its dynamic range, scaling of a given structure to optimize its dynamic range, and synthesis of structures that have good dynamic range.

A. Measuring Signal Magnitudes

In order to maximize the signal handling capability of a filter, and thus its dynamic range, one must design the filter so that the maximum signal magnitude at the output of each integrator is as large as the amplifier would allow without incurring significant distortion due to clipping or slew-rate limiting. For a given design, this signal maximization can be always achieved through the process known as scaling. Before we discuss scaling, however, we must decide on a mathematical measure for signal magnitude.

The choice of a measure for the magnitude of $x_i(s)$

$$x_i(s) = f_i(s)u(s)$$

depends strongly on the filter application and in particular on what is known about the input signal $u(s)$. Two cases are of special interest. The first concerns filters for which the input signal is known to consist primarily of a sinusoid of known peak amplitude M_u and of frequency in a given range; $\omega \in (\omega_a, \omega_b)$. In this case of a swept-frequency input the natural measure for the magnitude of $x_i(j\omega)$ is its absolute value

$$|x_i(j\omega)| = M_u|f_i(j\omega)|.$$

Thus the maximum signal magnitude at the output of integrator i is

$$|x_i(j\omega)|_{\max} = M_u \cdot \max|f_i(j\omega)|, \qquad \omega \in (\omega_a, \omega_b) \quad (31)$$

which is an L_∞ norm on the frequency response and is denoted $\|x_i(j\omega)\|_\infty$. This type of measure is easy to evaluate and has traditionally been used for scaling analog filters [10], [17], [18]. Its usefulness, however, is limited because of the inherent assumption of a swept-frequency input.

The second special case of interest is that where the power spectrum of the input signal, $P_u(\omega)$, is known, enabling us to find the power spectrum of $x_i(s)$ as

$$P_{x_i}(\omega) = P_u(\omega)|f_i(j\omega)|^2.$$

Here an appropriate measure for the magnitude of $x_i(s)$ is its rms value, or L_2 norm

$$\|x_i(j\omega)\|_2 = \sqrt{\int_{-\infty}^{\infty} P_{x_i}(\omega)\, d\omega}. \quad (32)$$

Assuming that the input power spectrum is white with density M_u^2 then

$$\|x_i(j\omega)\|_2 = M_u\|f_i(j\omega)\|_2 \quad (33)$$

where the L_2 norm of $f_i(j\omega)$ is given by

$$\|f_i(j\omega)\|_2 = \sqrt{\int_{-\infty}^{\infty} |f_i(j\omega)|^2\, d\omega}. \quad (34)$$

It is believed that L_2 measures of signal magnitude apply to a much wider class of filter problems than L_∞ measures.[2]

B. Noise

In continuous-time analog filters, noise is contributed by all active devices and resistors, and interfering signals are coupled into the circuit in various ways. One can usually treat the overall effect as equivalent to injecting noise only at the inputs of integrators. It is also usually reasonable to assume that these noise sources are independent of each other.

Noise signals injected at integrator inputs can be modeled by $\epsilon(s)$ in (6) and thus the functions $\{g_i(s)\}$ give the gain to the filter output for each of the input noise signals. If we assume that the noise signals all have white spectra with equal densities N_i^2, then the output noise will have a power spectrum

$$P_{no}(\omega) = N_i^2 \sum_i |g_i(j\omega)|^2. \quad (35)$$

Thus the *noise gain* of the filter is $\Sigma_i|g_i(j\omega)|^2$. For each realization of a given filter one can evaluate the noise gain function and use it for comparison. One can also obtain the rms noise level at the output by taking L_2 norms

$$\|P_{no}(\omega)\|_2 = N_i\sqrt{\int_{-\infty}^{\infty} \sum_i |g_i(j\omega)|^2\, d\omega}$$

$$= N_i\sqrt{\sum_i \|g_i(j\omega)\|_2^2} \quad (36)$$

Thus we can use $\Sigma_i\|g_i\|_2^2$, which is the output noise power obtained when all integrators have white nosie of unit power spectral density, as a figure of merit for comparing the noise performance of different realizations.

C. Scaling

For a given design, one is generally free to set the signal levels at integrator outputs arbitrarily by scaling operations. If too high a level is chosen, the amplifier will occasionally clip or slew-rate limit, while if too low a level is chosen the ratio of signal to noise will be low. We shall be interested in scaling so that the maximum signal magnitude at the output of each amplifier is equal to that that the amplifier is capable of supporting, denoted M. It should be noted, however, that the value of M depends on the type of norm (L_∞ or L_2) used to measure signal magnitude. For the commonly used L_∞ norms, M is simply determined from amplifier specifications. The determination of M is more involved when L_2 norms are used [14] and will not be pursued here.

Scaling can be performed on the circuit implementation, on the signal-flowgraph representation, or on the

[2] To accommodate signals that do not have white spectra one may include a frequency weighting function $W(\omega)$ in the definition of the L_2 norm in (34).

$\{A, b, c, d\}$ system description. Here we shall consider the latter. Scaling is achieved by changing the set $\{f_i(s)\}$ to a new set $\{\tilde{f}_i(s)\}$ which differ only by constant factors, that is

$$\tilde{f}_i(s) = \alpha_i f_i(s) \tag{37}$$

so that the magnitudes of $\{\tilde{x}_i(s)\}$ are

$$\|\tilde{x}_i\| = M, \qquad \forall i. \tag{38}$$

It follows that the scaling constants must be

$$\alpha_i = \frac{M}{M_u}\frac{1}{\|f_i\|} \tag{39}$$

and the scaled f functions will have the norms

$$\|\tilde{f}_i\| = \frac{M}{M_u}. \tag{40}$$

In many cases precise values of M_u and M may not be known. A convenient assumption in such a case is $M_u = M$ which results in

$$\alpha_i = \frac{1}{\|f_i\|} \tag{41}$$

and

$$\|\tilde{f}_i\| = 1. \tag{42}$$

Physically speaking this implies that for the particular norm chosen the scaled filter will be able to accommodate input signals as large as those allowed at amplifier outputs.

We would next like to know the effect of scaling on filter performance figures, in particular output noise and sensitivity, and on $\{A, b, c, d\}$. Toward that end we note that scaling is achieved by multiplying the vector f by a diagonal matrix T having the scaling factors $\alpha_1, \alpha_2, \cdots, \alpha_n$ as its elements

$$\tilde{f}(s) = Tf(s). \tag{43}$$

Thus, in terms of F we have

$$\tilde{F} = TF. \tag{44}$$

Now using (16) yields

$$\tilde{G} = T^{-1}G \tag{45}$$

which results in the scaled g functions

$$\tilde{g}(s) = T^{-1}g(s). \tag{46}$$

It follows that the noise gains are scaled by the inverse factors $(1/\alpha_1), (1/\alpha_2), \cdots, (1/\alpha_n)$. This is a very interesting result: by scaling the signal gains so that the output signal levels are maximized we automatically reduce the noise gains by the same factors. Thus scaling maximizes the dynamic range of a given design.

It can be easily shown that scaling according to (43) results in the parameters $\{\tilde{A}, \tilde{b}, \tilde{c}, \tilde{d}\}$ of the scaled system given by

$$\{\tilde{A}, \tilde{b}, \tilde{c}, \tilde{d}\} = \{TAT^{-1}, Tb, T^{-1}c, d\}. \tag{47}$$

Thus, $\tilde{A}_{ij} = (\alpha_i/\alpha_j)A_{ij}$, $\tilde{b}_i = \alpha_i b_i$, and $\tilde{c}_i = (c_i/\alpha_i)$. It follows that the structure remains unchanged. Also, using (19)–(23) shows that the sensitivities to $\{A, b, c, d\}$ and to integrator gains do not change by scaling. Note, however, that because A_{ij} and b_i change, the integrator gains will change and thus the sensitivities to op amp nonidealities will change. It turns out, however, that well scaled structures tend to have low integrator gains and hence low sensitivities to op amps.

To illustrate the scaling process consider the third-order filter that we have been using as a "running example". Assume that we expect the input signal to have a constant (white) spectral density of 1 $V/\sqrt{rad/s}$. Choosing L_2 norms for measuring signals we obtain for the three f functions

$$\|f_1\|_2 = 1.618 \quad \|f_2\|_2 = 0.8862 \quad \|f_3\|_2 = 0.7236.$$

Now if we decide, for instance, that a 1.5 V rms level is acceptable at the output of each integrator [14] we may scale $\{f_i(s)\}$ according to

$$\alpha_i = \frac{1.5}{\|f_i\|}.$$

Thus, for instance, $f_3(s)$ changes to

$$\tilde{f}_3(s) = \frac{1.5}{0.7236} f_3(s) = \frac{1.036}{e(s)}.$$

Note that g_1 increased, but then the unscaled filter would not have been able to tolerate the 1 $V/\sqrt{rad/s}$ signal at the input because x_1 would have been too large. Thus we scaled f_1 down to allow full signal swing, and f_2 and f_3 up to reduce g_2 and g_3 and thus noise.

Note that this approach to scaling is more general (since it is applicable to arbitrary structures), more exact (because it uses a realistic statistical model for the input signal rather than a swept-frequency model), and easier to understand than that presented in [10].

D. Structures with Optimum Dynamic Range

Scaling optimizes the dynamic range of a given structure, but some structures are inherently better for dynamic range than others. This subsection adapts for analog filters the results of [16] which show how to construct a state-space digital filter with optimum dynamic range. Such a structure has the lowest $\Sigma_i \|g_i\|_2^3$ over all L_2-scaled filters and thus has the highest dynamic range possible.

The results follow from an analysis of the behaviour of two matrices, K and W, which give correlation among $\{f_i(j\omega)\}$ and $\{g_i(j\omega)\}$, respectively. They are defined by

$$K_{ij} \triangleq g_i \cdot f_j \tag{48}$$

$$W_{ij} \triangleq g_i \cdot g_j \tag{49}$$

where $\cdot$ denotes an inner product. Although any inner product may be used without affecting the results of [16] we shall select the inner product that yields squared L_2 norms for the diagonal elements, K_{ii} and W_{ii}. Thus we use

$$f_i \cdot f_i \triangleq \int_{-\infty}^{\infty} \bar{f}_i(j\omega) f_j(j\omega)\, d\omega. \tag{50}$$

Mullis and Roberts [16] investigated the dynamic range of structures by examining the product $K_{ii}W_{ii} = \|f_i\|_2^2 \|g_i\|_2^2$. This product is not affected by scaling but it does change from one structure to another. If one scales a structure with a given $\Sigma_i K_{ii}W_{ii}$ in order to get $\tilde{K}_{ii} \equiv \|\tilde{f}_i\|_2^2 = 1\ \forall i$, then the output noise of the L_2-scaled filter is $\Sigma_i \tilde{W}_{ii} = \Sigma_i \tilde{K}_{ii}\tilde{W}_{ii} = \Sigma_i K_{ii}W_{ii}$. The figure $\Sigma_i K_{ii}W_{ii}$, therefore, shows the inherent dynamic range of the structure.

Mullis and Roberts [16] show how to use linear transformations to generate realizations having minimum $\Sigma_i K_{ii}W_{ii}$. The resulting structure has interesting properties. By suitable scaling it may be made to satisfy two conditions

$$\boldsymbol{K} = \boldsymbol{W}$$

and $K_{ii} = K_{jj}\ \forall i, j$. The condition $\boldsymbol{K} = \boldsymbol{W}$ implies a sort of self-duality, because it says that the interrelationships among $\{f_i\}$ are the same as those among $\{g_i\}$. This kind of symmetry appears also in some minimum-sensitivity structures [14], and bears a thought-provoking resemblance to a reciprocity condition.

The derivation of [16] for minimum $\Sigma_i K_{ii}W_{ii}$ relies on the invariance of the eigenvalues of $\boldsymbol{KW}$. These eigenvalues can be determined from the product $\boldsymbol{KW}$ for any realization of the given transfer function. Denoting these eigenvalues μ_i^2 (they have also been called "principal values" and "second-order modes") the sum $\Sigma_i K_{ii}W_{ii}$ for the realization with optimum dynamic range is given by

$$\sum_i K_{ii}W_{ii} = \frac{1}{n}\left(\sum_i \mu_i\right)^2. \tag{51}$$

This figure represents the lowest possible noise obtainable for a given transfer function $t(s)$ and thus serves as a target for comparing the dynamic range of a given realization.

The realization having optimum dynamic range turns out to be rather difficult to obtain (it requires an iterative time-consuming procedure) and its structure is fully dense (that is, has nonzero values for every $\{\boldsymbol{A}, \boldsymbol{b}, \boldsymbol{c}, d\}$ coefficient). One might, therefore, wish to find a relatively sparse suboptimum system (Section V) as long as the dynamic range performance sacrificed by so doing is not excessive.

E. Orthogonality and Angles

IF synthesis is based on the selection of n linearly independent functions to serve as $\{f_i(s)\}$ or $\{g_i(s)\}$. The question arises as to the effect on performance of selecting two or more functions that exhibit "near dependency". A partial answer to this question is found by examining the relationship in (16). Obviously two f functions that are "close" to each other will cause the g functions to grow in value and this in turn results in increased sensitivities and noise (Section V). At this point we wish to quantify this notion of near dependence.

The concept of inner product introduced above may be used to define "angles" among $\{f_i(j\omega)\}$ vectors. As a particularly interesting case, two (nonzero) vectors f_i and f_j are said to be orthogonal when $f_i \cdot f_j = 0$. In general, the angle between two vectors is given by ϑ

$$\vartheta \triangleq \cos^{-1}\left[\frac{f_i \cdot f_j}{\|f_i\|_2 \|f_j\|_2}\right]. \tag{52}$$

This definition has the natural geometric properties for angles: in particular if the angle between two vectors is 0, then they are aligned (i.e., one is just a scalar multiple of the other).

Using the concept of angle we can say that a system "almost" has linear dependency among its $\{f_i\}$ if the angle between two $\{f_i\}$ is very small (or, better, if the angle between some f_i and the subspace spanned by the others is very small). Application and illustration of this concept is given in the next section in the context of design examples.

TABLE I
TRANSFER FUNCTION AND OTHER PARAMETERS FOR DESIGN EXAMPLE

Polynomial:	Natural Modes	Attenuation Poles	Attenuation Zeros	Numerator of [dt(s)/ds]
Leading coefficient:	1210.19	5.31436	3896.185	12862.8
List of roots:	-.0681354± j.916348	0	± j.909524	-0.0357517± j.741621
	-.06388± j.788556	0	± j.98919467	-.0611769± j.851543
	-.0232875± j.710193	± j1.25008	± j.796951	-.039558± j.9689114
	-.0262875± j1.00448	± j.399736	± j.723907	.030864± j1.42125
				.0057± j.3135
				-.937486
				.95568
				0

V. APPLICATIONS

In this section the IF method is employed in the synthesis and analysis of a number of realizations for an eighth-order active bandpass filter. The sensitivity and noise properties of these realizations are evaluated and compared to theoretical lower bounds. It is shown how one can alter the structure of known realizations as well as synthesize new structures to approach these lower bounds.

The filter to be investigated meets an arithmetically symmetric set of specifications [10]:

passband: 1 to 1.4 kHz with 0.4-dB ripple and unity gain;

stopbands: $\leqslant 700$ Hz and $\geqslant 1700$ Hz with 50-dB minimum attenuation.

We will work throughout with a frequency normalized version in which the upper passband edge is 1 rad/s. Table I lists the roots and leading coefficients of the various polynomials that characterize the eighth order transfer function meeting these specifications. Also shown are the numerator roots of $(dt(s))/ds$ which are needed for the derivative-based design described below. All the realizations presented will be scaled so that $\|f_i\|_2 = 1, \forall i$.

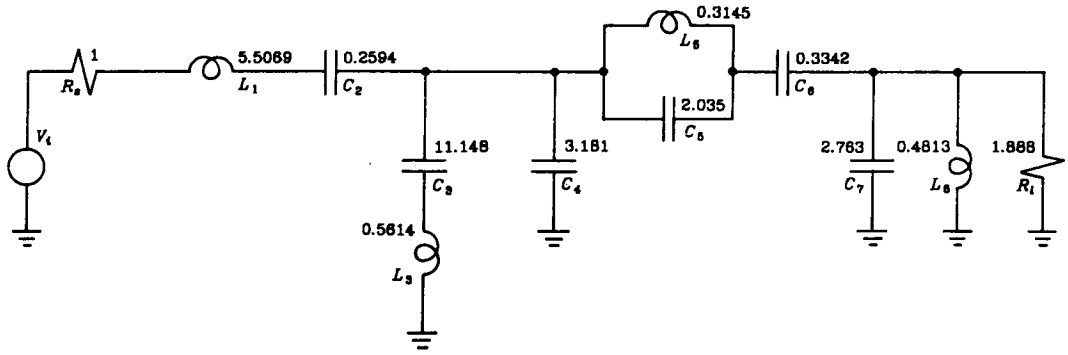

Fig. 9. An eighth-order *LC* ladder bandpass filter to be simulated.

TABLE II
ZEROS OF THE INTERMEDIATE TRANSFER FUNCTIONS OF THE LADDER OF FIG. 9

Intermediate function	Numerator roots of intermediate function
$\frac{I_{L1}}{V_i}$	-.022528± j.73095 -.04425± j.854146 -.02402± j.9829337 0
$\frac{V_{C2}}{V_i}$	$\frac{1}{s}(I_{L1}/V_i)$
$\frac{I_{L3}}{V_i}$	-.0467423± j.7641159 -.04381265± j.957335 0
$\frac{V_{C3}}{V_i}$	$\frac{1}{s}(I_{L3}/V_i)$
$\frac{V_{C4}}{V_i}$	± j.39974 -.046742± j.76412 -.043813± j.95733
$\frac{V_{C5}}{V_i}$	0.0 ± j.39974 -.095866± j.86193
$\frac{I_{L5}}{V_i}$	$\frac{1}{s}(V_{C5}/V_i)$
$\frac{V_{C6}}{V_i}$	± j.399736 -.095866± j.86193 ± j1.25008
$\frac{V_{C7}}{V_i}=t(s)$	0.0 ± j.39974 ± j1.25008
$\frac{I_{L8}}{V_i}$	$\frac{t(s)}{s}$

A. Design Based on LC Ladder Simulation

Fig. 9 shows an *LC* ladder realization of the eighth-order bandpass filter. It has ten reactive components and thus two "extra" states which must be discarded and eight independent states selected for simulation. However, apart from ensuring linear independence care must be exercised in this selection process [14], [19], or all the advantages of ladder simulation will be lost, as illustrated below.

Analysis of the ladder using FILTOR 2 [20] gives its intermediate transfer functions, listed in Table II.[3] As a first attempt at simulating this filter we discard states V_{C2} and V_{C4}. The transfer functions to the remaining eight states $(I_{L1}, I_{L3}, V_{C3}, V_{C5}, I_{L5}, V_{C6}, V_{C7}, I_{L8})$ constitute $\{f_i(s)\}$ to be used in the IF synthesis procedure. The resulting realization has the noise characteristics

$$\left[\sum_i |g_i(j\omega)|^2\right]$$

plotted in Fig. 10 and labeled Ladder 1. The output noise due to each of the eight integrators

$$\|g_i\|_2^2 =$$

$$[7.78 \quad 9.76 \quad 66.2 \quad 345.5 \quad 9.76 \quad 406.5 \quad 49.7 \quad 7.8]$$

and so the total output noise for this L_2-scaled filer is $\Sigma_i \|g_i\|_2^2 = 902.9$.

For comparison purposes, the total output noise for the optimum-dynamic-range realization of this filter was evaluated using (51) and found to be 67.4. Thus, this ladder simulation has more than 5 dB of noise above the optimum. Furthermore, the results above indicate that integrators 4 and 6 generate most of the total noise. Examination of the A matrix (not shown here because of space limitations) shows that the first two rows contain fairly large elements in columns 4 and 6. This suggests that f_4 and f_6 are nearly equal and that subtraction is being used to form inputs sx_1 and sx_2. That there is excessive correlation between states 4 and 6 was confirmed by evaluating the angle between f_4 and f_6 using (52). The angle was found to be 21°. Furthermore, sensitivity analysis showed that the sensitivities to integrators 4 and 6 are between 10 and 15 times greater than the optimum value.

A much better simulation of this ladder was obtained by replacing the state variables V_{C3} and V_{C6} by V_{C2} and V_{C4}. The noise and worst-case relative sensitivity of the resulting realization are plotted in Figs. 10 and 11, respectively, and labelled Ladder 2. It was found that for this realization all A_{ij} are less than 1 in magnitude and that all integrator noise contributions are comparable in value, with the total

[3] It might be observed that many of the roots of the polynomials are quite close to the roots of the derivative of $t(s)$ (listed in Table I), an interesting observation in view of the result in (28) for minimum-sensitivity filters.

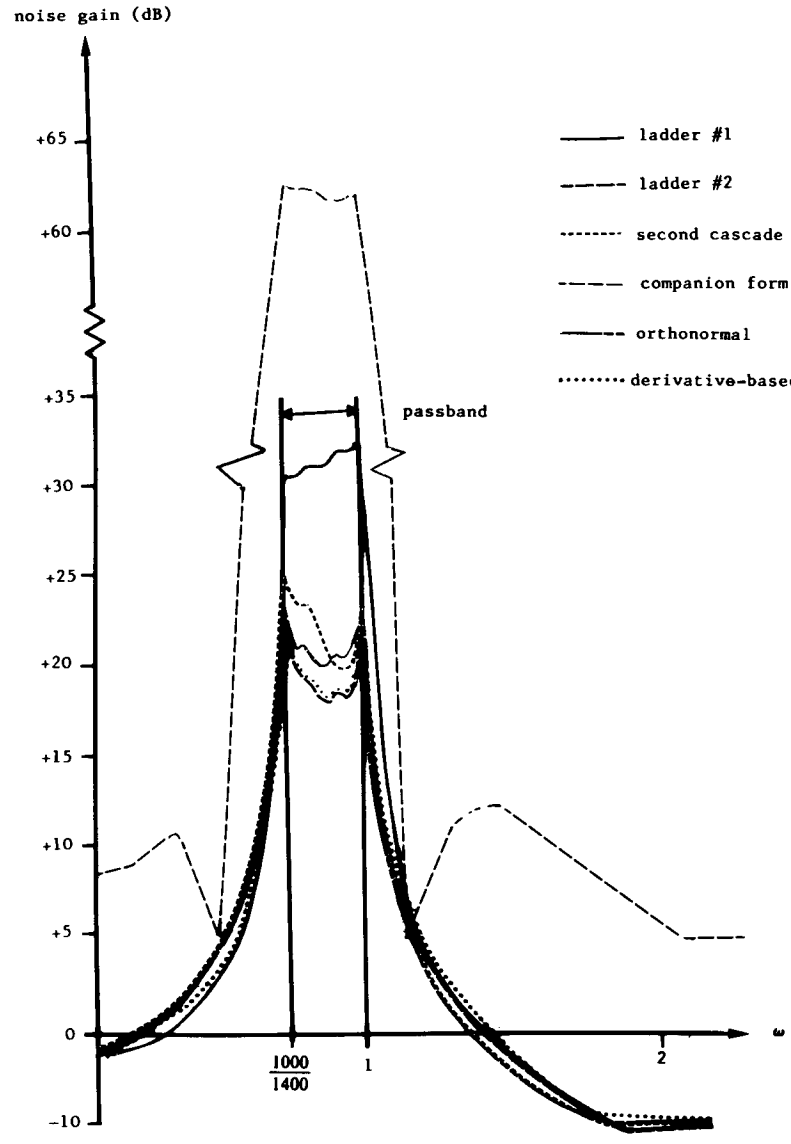

Fig. 10. The total output noise, $\Sigma_i |g_i(j\omega)|^2$, for the various realizations considered.

noise being 72.7 which is within 0.4 dB of the optimum. Also, from Fig. 11 we observe that over the passband the worst case sensitivity is near the optimum value of 1/8. Thus the filter is approximately equally sensitive to each of its eight integrators in the passband. Over most of the stopbands, however, the sensitivity is about 1/2, implying that a pair of integrators dominate performance.

Finally, we note that this canonic realization with near optimum passband performance has a fairly sparse $\boldsymbol{A}$ matrix, with only 27 of the 81 elements being non-zero, and that its $\boldsymbol{b}$ and $\boldsymbol{c}$ have one element each.

B. Cascade Design

The cascade design investigated uses four two-integrator loops connected in cascade with zeros formed by summing the two outputs of each section at the inputs of integrators in later sections. Denoting the transfer function of the jth section Γ_j, the $\{f_i(s)\}$ appearing in the kth section are

$$f_i(s) = \left[\prod_{j<k} \Gamma_j\right] \frac{1}{e_k(s)}$$

$$f_{i+1}(s) = \left[\prod_{j<k} \Gamma_j\right] \frac{s}{e_k(s)}$$

where $e_k(s)$ is the denominator polynomial of the kth section.

Fig. 12 shows a particular choice of factors Γ_j for $t(s)$, that is, a particular "pairing and ordering" [10], [17]: each singularity is labelled with the index number of the section (Γ) which realizes it. This is done following the rule-of-thumb in [10], [17]. In particular, the sections are ordered to have successively higher Q factors from input to output, with the low-pass and high-pass sections alternated. The resulting realization, obtained using IF synthesis, was found

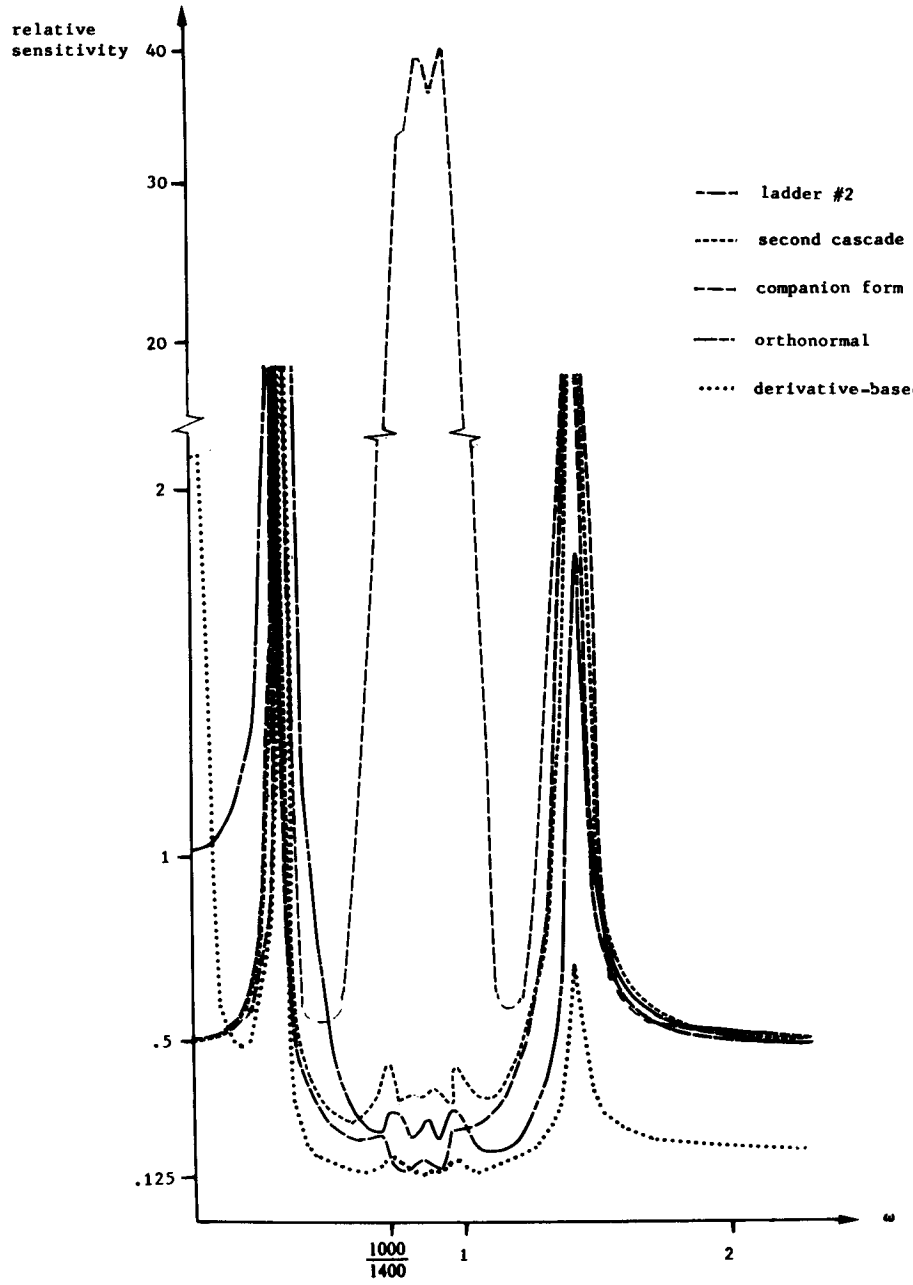

Fig. 11. Worst-case integrator sensitivity $S_{\gamma,\infty}(\omega)$ for the various realizations considered.

to have a total output noise of 125.5 which is 3 dB higher than the optimum.

The ordering used above obviously lacks symmetry. On the other hand, the dual roles of $\{f_i(s)\}$ and $\{g_i(s)\}$ suggest that if a particular design is good then its dual must also be. Here by dual we mean a new system derived by interchanging $\{f_i\}$ and $\{g_i\}$ of a system, which interchanges inputs and outputs in a state-space structure. Therefore, we propose a different ordering: that the highest-Q sections of a cascade filter be placed in the middle of the structure and the low-Q sections on the outside. Another cascade realization was designed following this new ordering rule with the ordering as indicated in Fig. 13. The noise and sensitivity performance of the resulting realization are plotted in Figs. 10 and 11. The total noise was found to be 109.7, lower than that of the first cascade with the spectrum slightly "peakier" than that of the good ladder simulation.

For this cascade design we observe that $S_{\gamma,\infty} \simeq 1/2$ over the passband and most of the stopbands. Thus while the stopbands performance is similar to that of the ladder simulation the passband sensitivity is higher by a factor of $(n/2)$. This is because in the cascade two integrators dominate performance in any frequency region.

C. A Companion-Form Design

For a companion-form realization, Fig. 14, the $\{f_i(s)\}$ are simply $\{s^{i-1}/e(s)\}$. The noise and sensitivity perfor-

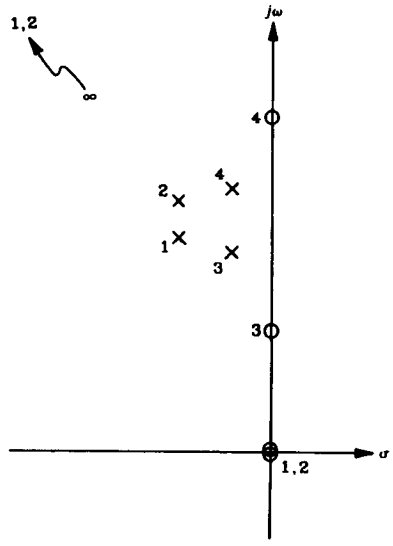

Fig. 12. A sketch of the s-plane showing a particular pole–zero pairing and section ordering for the cascade design of the eighth-order filter example.

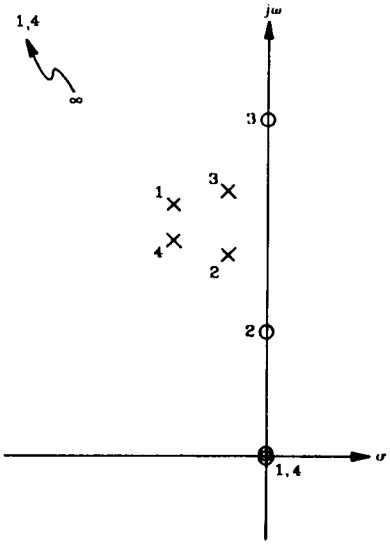

Fig. 13. An alternative section ordering that results in a cascade design with better performance than that obtained following the usual practice.

mance of the resulting system are shown in Figs. 10 and 11 and are obviously much worse than those for any of the other realizations attempted. The poor performance is due to the "near dependence" of some of the $\{f_i(s)\}$. Specifically, $K_{13} \simeq K_{24} \simeq K_{i,i+2} \simeq 0.98$ which means that every f_i is 98 percent correlated with f_{i+2} and f_{i-2}, or separated by an angle of only 13° from its second derivative.

D. An Orthonormal Realization

Since realizations in which some of the f functions exhibit near dependencies feature increased noise and sensitivity, it would be interesting to examine a realization in which all $\{f_i(s)\}$ are orthogonal. We call such a system, when L_2-scaled such that $\|f_i\|_2 = 1 \ \forall i$, an *orthonormal* realization. One can be obtained from any set of independent $\{f_i(s)\}$ by using the Gram–Schmidt orthonormalization procedure [21].

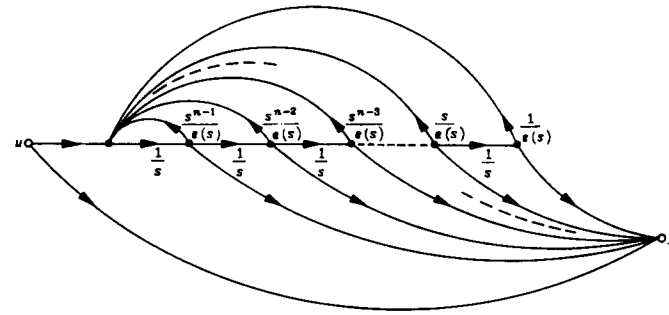

Fig. 14. Signal-flow graph representation of the companion-form realization.

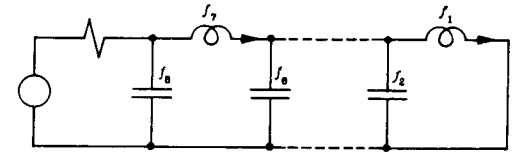

Fig. 15. A singly-terminated LC ladder that realizes the poles of the eighth-order filter. It turns out that the orthonormal realization is a simulation of this network.

TABLE III
INTERMEDIATE FUNCTIONS FOR THE ORTHONORMAL REALIZATION

Function	Leading coefficient	List of roots
f_1	0.00165	-
f_2	0.002065	0
f_3	0.01105	± j0.8033
f_4	0.01277	0.± j.82457
f_5	0.0677	± j0.7414, ± j0.93742
f_6	0.08044	0, ± j0.75018, ± j0.94929
f_7	0.30171	± j.7126, ± j.8335, ± j.9848
f_8	0.34	0, ± j0.7225, ± j0.8561, ± j0.9943

Starting from the set $\{f_i = s^{i-1}/e(s)\}$ (which is the one realized in the companion form) we obtain for the orthonormal system the IF's show in Table III. It is interesting to note that these $\{f_i(s)\}$ have notches in the filter passband. Since sensitivities are proportional to $\{f_i(s)\}$ it follows that various sensitivities go to zero in the passband. Note that both magnitude and phase sensitivities are forced to zero, where only magnitude sensitivity is zero in a ladder. The net effect is, however, not as good as this would suggest because not all sensitivities are forced to zero simultaneously and those that are not zero become larger than they would be for, say, a minimum-sensitivity structure.

For the orthonormal realization the total output noise is $\Sigma_i \|g_i\|_2^2 \simeq 100$, slightly better than the cascade design and within about 2 dB of the optimum. The resulting system

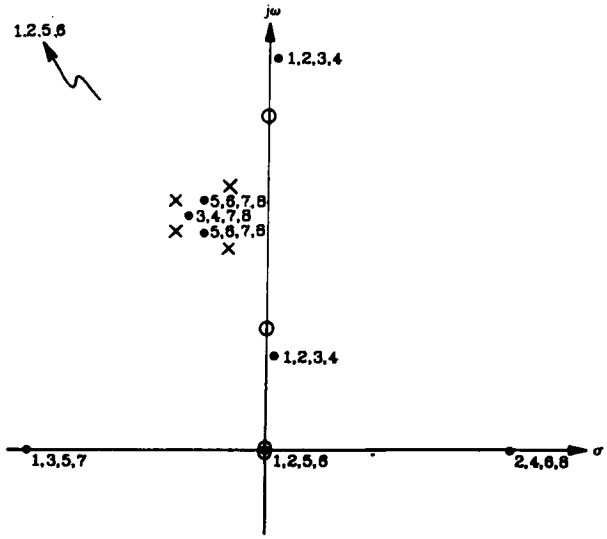

Fig. 16. Assignment of derivative roots to $\{f_i(s)\}$.

has a sparse A matrix and in fact turns out to be a simulation of a singly-terminated LC ladder network that realizes the filter poles (Fig. 15). The noise and sensitivity (Figs. 10 and 11) are comparable to those for a good cascade design. Finally, we note that the orthonormal property may be useful in adaptive filtering.

E. A Derivative-Based Design

From equation (28) we see that if the minimum-sensitivity realization exists then its $\{f_i(s)\}$ must divide $t'(s)$. In an attempt to find this realization, or one close to it, we choose various sets $\{f_i(s)\}$ by combining the prime factors of $t'(s)$, and investigate the resulting system.

Fig. 16 is a sketch of the s-plane showing roots of both $t(s)$ and $t'(s)$ (see also Table I). It shows with each root of the numerator of $t'(s)$ a list of the index numbers i of the $\{f_i(s)\}$ that contain that root for a particular design. This particular choice of $\{f_i(s)\}$ was made to have a number of symmetries, one of which gives a sort of "reciprocity" and one of which tends to force the system to have substructures resembling the minimum-sensitivity biquads discussed elsewhere [15].

We expect some sort of "reciprocity" to be useful because we know that, because of the dual roles of $\{f_i\}$ and $\{g_i\}$, taking the dual of a good system ($\{\tilde{f}_i\} = \{g_i\}$) should yield another good one. That in turn suggests that if a unique best system exists it must be self-dual. The $\{f_i(s)\}$ in Fig. 16 are so chosen that the factors of $t'(s)$ missing from any $f_i(s)$ (which would be the factors of $g_i(s)$ if this happened to be the minimum-sensitivity realization) appear in f_{9-i}, that is, $f_1 f_8 = f_2 f_7 = f_3 f_6 = f_4 f_5 = t'(s)$.

We have also chosen factors so that all $\{f_i(s)\}$ are bandpass in appearance, that is we have paired corresponding factors from above and below the band centre. This was done because some preliminary results in our current investigation of minimum-sensitivity structures indicate that for a bandpass filter, the minimum sensitivity realization must be composed of bandpass subfilters.

The resulting realization has a total output noise of 73.96, very close to that of the best ladder simulation circuit. The output noise spectrum, shown in Fig. 10, is also similar to that of the ladder simulation. Most interesting, however, is the sensitivity performance, plotted in Fig. 11. While the lower-stopband performance is mediocre, this filter is superior to any other in the upper stopband and in the passband, where it is close to having minimum-sensitivity performance ($S_{\gamma,\infty} = 1/8$). Unfortunately, however, the system matrices are fairly dense.

VI. Conclusions

A simple procedure has been presented for the synthesis of state-space analog filters. The method is based on the selection of an appropriate set of intermediate transfer functions. It has been shown that the filter sensitivity and dynamic range properties are easily determined from its intermediate functions. Therefore, it is possible to optimize sensitivity and dynamic range by the appropriate choice of intermediate functions. A number of the results presented should aid in this selection process.

Application of the IF theory has been demonstrated via a comparative study of analog filter structures in the context of a bandpass filter design. In doing so, we have shown a new and very general technique for performing ladder simulation, suggested an improvement in cascade design, uncovered an interesting property of singly terminated all-pole ladders, and derived a new design superior in the upper stopband to any other. In conclusion, we believe that the intermediate function method yields valuable design guidance and theoretical insights.

References

[1] R. Gregorian, K. W. Martin and G. C. Temes, "Switched-capacitor circuit design," *Proc. IEEE*, vol. 71, pp. 941–966, Aug. 1983.

[2] Y. Tsividis, M. Banu and J. Khoury, "Suitability of MOS circuits for integrated high performance active filters," in *Proc. 1984 Int. Symp. Circuits Syst.*, Montreal, Canada, pp. 928–931, May 1984.

[3] R. F. MacKay and A. S. Sedra, "Generation of low-sensitivity state-space active filters," *IEEE Trans. Circuits Syst.*, vol. CAS-27, pp. 863–870, Oct. 1980.

[4] C. A. Desoer and E. S. Kuh, *Basic Circuit Theory*. New York: McGraw-Hill, 1969, ch. 12.

[5] R. W. Newcomb, *Active Integrated Circuit Synthesis*. Englewood Cliffs, NJ: Prentice-Hall, 1968.

[6] W. M. Snelgrove and A. S. Sedra, "A novel synthesis method for state-space active networks," in *Proc. Midwest Symp. Circuits and Systems*, Toledo, OH, pp. 196–200, Aug. 1980.

[7] J. Tow, "Active-*RC* filters—A state-space realization," *Proc. IEEE*, vol. 56, pp. 1137–1139, June 1968.

[8] L. C. Thomas, "The Biquad: Part 1—Some practical design considerations," *IEEE Trans. Circuit Theory*, vol. CT-18, pp. 350–357, May 1971.

[9] J. Tow and Y. L. Kuo, "Coupled-biquad active filters," in *1972 IEEE Int. Symp. on Circuit Theory*, North Hollywood, CA, pp. 164–168, 1972.

[10] A. S. Sedra and P. O. Brackett, *Filter Theory and Design: Active and Passive*. Portland, OR: Matrix, 1978.

[11] R. Seviora and M. Sablatash, "A Tellegen's theorem for digital filters," *IEEE Trans. Circuit Theory*, vol. CT-18, pp. 201–203, Jan. 1971.

[12] H. J. Orchard, "Inductorless filters," *Electron. Lett.*, vol. 2, pp. 224–225, June 1966.

[13] M. S. Ghausi and K. R. Laker, *Modern Filter Design*. Englewood Cliffs, NJ: Prentice-Hall, 1981.

[14] W. M. Snelgrove, "Intermediate-function synthesis," Ph.D. dissertation, Univ. Toronto, Toronto, Ont., Canada, 1982.

[15] W. M. Snelgrove and A. S. Sedra, "State-variable biquad with optimum integrator sensitivities," *Proc. Inst. Elect. Eng.*, vol. 128, part G, no. 4, pp. 173–175, Aug. 1981.

[16] C. T. Mullis and R. A. Roberts, "Synthesis of minimum-roundoff noise fixed-point digital filters," *IEEE Trans. Circuits Syst.*, vol. CAS-23, pp. 551–562, Sept. 1976.
[17] G. S. Moschytz, *Linear Integrated Networks: Design*. New York: Van Nostrand Reinhold, 1975.
[18] W. M. Snelgrove and A. S. Sedra, "Optimization of dynamic range in cascade active filters," in *1978 IEEE Int. Symp. Circuits Syst.*, New York, pp. 151–155, May 1978.
[19] D. Johns, "State-space filters based on LC ladder simulation," M.A.Sc. thesis, Univ. Toronto, Toronto, Ont., Canada, 1983.
[20] W. M. Snelgrove, "FILTOR 2—A computer-aided filter design package," Univ. Toronto, Toronto, Ont., 1981.
[21] D. G. Luenberger, *Optimization by Vector Space Methods*. New York: Wiley, 1978.

✠

W. Martin Snelgrove was born in Kitwe, Zambia, in October 1954. He received the B.A.Sc., degree in chemical engineering in 1975, and the M.A.Sc. and the Ph.D. degrees in electrical engineering from the University of Toronto, Toronto, Ont., Canada, in 1977 and 1982, respectively.

In 1982 he worked at the Instituto Nacional de Astrofisica, Optica y Electronica, Tonantzintla, Mexico, as a visiting investigator. Since then he has been at the University of Toronto as an Assistant Professor. He is involved in research projects in the University's Computer Systems Research Institute and its VLSI Research Group, primarily in the areas of CAD on multiprocessors and high-frequency integrated filters.

Adel S. Sedra (M'66–SM'82–F'84) was born in Egypt on November 2, 1943. He received the B.Sc. degree from Cairo University, Egypt, in 1964, and the M.A.Sc. and Ph.D. degrees from the University of Toronto, Canada, in 1968 and 1969 respectively, all in electrical engineering.

From 1964 to 1966, he served as Instructor and Research Engineer at Cairo University. Since 1969 he has been on the staff of the University of Toronto where he is currently a professor in the Department of Electrical Engineering, and Executive Director of the Microelectronics Development Centre. He has also served as a consultant to industry and government in Canada and the U.S., and was President of Electrical Engineering Consociates Ltd., a research and design consulting company, for the period 1979–1981. He has served the IEEE and in particular the Circuits and Systems Society in a variety of roles, including: Chairman of Local Arrangements for the 1973 International Symposium on Circuit Theory; Member of the Program Committee of the 1978 ISSCC; Associate Editor of the IEEE TRANSACTIONS ON CIRCUITS AND SYSTEMS (1981–1983); Program Chairman of the 1984 ISCAS; Member of the Administrative Committee of the IEEE Circuits and Systems Society (1984–1987); Circuits and Systems Editor of the *IEEE Circuit and Devices Magazine* (1985–); Co-Guest Editor of the Joint Special Issue of the *IEEE* TRANSACTIONS ON CIRCUITS AND SYSTEMS and the IEEE JOURNAL OF SOLID-STATE CIRCUITS on VLSI Analog and Digital Signal Processing (February 1986).

Dr. Sedra's research work has been in the area of active-*RC* and MOS switched-capacitor filters. He has published about eighty papers and two books: *Filter Theory and Design: Active and Passive* (co-authored with Peter Brackett, matrix Publishers, 1978) and *Microelectronic Circuits* (co-authored with K. C. Smith, Holt, Rinehart, and Winston, 1982). One of his papers (co-authored with R. B. Datar) is the winner of the 1984 IEEE Circuits and Systems Society Darlington Award.